

Measurement of the π^+p and π^-p Polarization Parameters at 100 GeV/c

I. P. Auer, D. Hill, B. Sandler,^(a) and A. Yokosawa
Argonne National Laboratory, Argonne, Illinois 60439

and

W. Brückner, O. Chamberlain, H. Steiner, and G. Shapiro
Lawrence Berkeley Laboratory, Berkeley, California 94720

and

A. Jonckheere and P. F. M. Koehler
Fermi National Accelerator Laboratory, Batavia, Illinois 60510

and

R. V. Kline, M. E. Law, and F. M. Pipkin
Harvard University, Cambridge, Massachusetts 02138

and

W. Johnson
Suffolk University, Boston, Massachusetts 02114

and

J. Snyder and M. E. Zeller
Yale University, New Haven, Connecticut 06520

(Received 24 May 1977)

We report measurements of the polarization parameters in π^+p and π^-p elastic scattering at an incident momentum of 100 GeV/c. The results cover the range $0.18 \leq -t \leq 1.4$ GeV² and are in agreement with current Regge-model predictions.

In the first experiment of its kind at Fermilab we have measured the polarization parameter $P(t)$ in the elastic scattering of mesons and protons from polarized protons. We present here the results for π^+p and π^-p scattering which were obtained at a beam momentum of 100 GeV/c over the range of the square of the four-momentum transfer $0.18 \leq -t \leq 1.4$ GeV².

While recent measurements of elastic differential cross sections in this kinematic region^{1,2} have confirmed phenomenological predictions of the s and t dependence of the dominant Pomeron amplitude,^{3,4} polarization measurements provide more stringent tests of present models because they are sensitive to interference between amplitudes. For example, a model in which Pomeron- and ρ -exchange contributions dominate predicts that $P(t)$ in πp scattering should be proportional to s^x with $x = \alpha_\rho(t) - \alpha_P(t)$, where s is the square of the total energy of the system, and $\alpha_\rho(t)$ and $\alpha_P(t)$ are the effective trajectories for the ρ - and Pomeron-exchange contributions, respectively. This s dependence is approximately $s^{-1/2}$ at small $|t|$.

This model also predicts that the mirror symmetry $P_{\pi^+p} \simeq -P_{\pi^-p}$ persists at high energies.³ In the region $0.6 \leq -t \leq 1.5$ GeV² the dominant amplitudes are strongly affected by shrinkage and absorption, resulting in small polarization values at high energies.⁵

The experiment was performed in the 3.5-mrad beam (M1) in the Meson Laboratory which had a size of 2×2 cm² and a divergence of ± 0.2 mrad at the target while transporting a momentum bite of $\pm 1\%$. The small divergence was necessary for kinematic separation of elastic from quasielastic events. In order to determine polarizations of ≈ 0.05 with high precision, we placed no components in the beam, enabling the apparatus to handle incident fluxes as large as 10^8 /sec.

The layout of the apparatus is shown schematically in Fig. 1. It consisted of a double-arm spectrometer capable of detecting both final-state particles with uniform acceptance over the range $0.25 \leq -t \leq 1.5$ GeV². The final-state trajectories were measured with eight planes of multiwire proportional chambers (PWC's) in

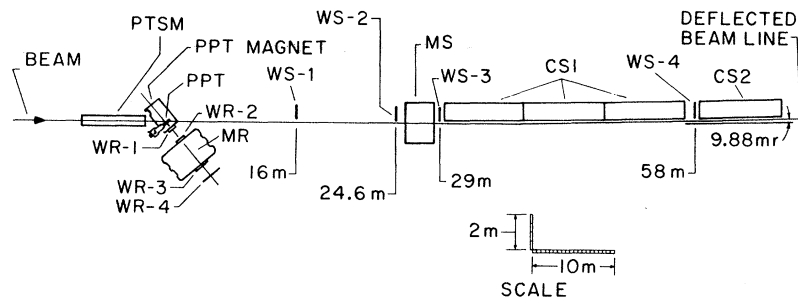


FIG. 1. Plan view of the apparatus. The magnet PTSM compensated for the beam deflection introduced by the PPT magnet. The magnetic-field line integrals of the analysis magnets MS and MR were 3.29 and 0.35 T·m, respectively.

each arm. In the recoil arm two pairs of x - y planes (WR-1, WR-2) were placed in front of a wide-gap analysis magnet (MR), and two pairs of x - v planes (WR-3, WR-4) behind it. The resulting measurement of the recoil momentum was accurate to $\pm 1.7\%$ at 500 MeV/ c ($t = -0.2$ GeV 2). In the forward arm two pairs of x - y planes (WS-1, WS-2) were located in front of an analysis magnet (MS), and a pair of x - u and x - v planes (WS-3, WS-4) behind it. The momentum of the forward particle was determined to an accuracy of $\pm 1\%$. Two Cherenkov counters (CS1, CS2), with thresholds just below kaon and proton response, respectively, were used to identify the scattered particle. The purity of the pion sample thus identified was better than 99%.

The polarized proton target (PPT) consisted of ethylene glycol maintained in a uniform magnetic field of 2.5 T at a temperature of 0.42°K. The target was 2.0×1.9 cm 2 in cross section and 8.2 cm long. The free-proton density was 0.072 g/cm 3 , comparable to that in liquid hydrogen. The target polarization was measured by standard NMR techniques every tenth spill and recorded on the data tapes. The average polarization of the free protons was 75%.

The number of incident particles was monitored indirectly by a three-counter telescope (MT) which looked back at the target from an angle of 100 mrad below the beam line, in the plane formed by the beam momentum and the target polarization. It was thus insensitive to the spin orientation of the target protons. The absolute normalization of MT was obtained at reduced beam intensities where the number of beam particles could be measured directly with a pair of additional counters just upstream of the target. The size and position of the final beam spot were monitored in several ways: by scaling the sig-

nals from the pole-tip veto counters (PT) above and below the target; by a profile monitor and a hole veto counter (H) in the beam just upstream of the target; and by a pair of counters at WS-2 which were spaced to monitor the tails on both sides of the unscattered beam.

The event trigger required at least one particle in each arm and no signal in any of the veto counters H or PT. In addition, kinematic constraints could be imposed on the final-state particles by combining the information from the PWC's with the help of matrix coincidences. The data presented here were taken with a fairly loose trigger which only required signals in WS-1 x and the x planes of the four recoil-arm PWC's.

The data were analyzed by reconstructing the polar and azimuthal scattering angles for each arm (θ_s , φ_s , θ_r , and φ_r), and the magnitude of the recoil particle momentum (p_r). Independent values of t were calculated from each of the measured quantities θ_s , θ_r , and p_r , and compared by forming a weighted average \bar{t} and the corresponding χ^2 . By use of φ_s , φ_r , and their combined measurement uncertainty $\delta\varphi$, the quantity $\Delta\varphi/\delta\varphi = (\varphi_s - \varphi_r)/\delta\varphi$ was calculated to judge the extent to which the two final-state particles and the incident particle were coplanar. By plotting events according to χ^2 and $\Delta\varphi/\delta\varphi$, "signal," "intermediate," and "background" regions were selected. The subtraction of the quasielastic background under the elastic peak was performed by normalizing the coplanarity distribution for events with large χ^2 so that the tails matched those of the coplanarity distribution for events with small χ^2 . The signal-to-background ratio varied from 15:1 at small $|t|$ to 7:1 at $t = -1.0$ GeV 2 , consistent with the results of a Monte Carlo simulation of elastic events from the free protons and quasielastic events from the bound pro-

TABLE I. Results for the polarization parameter $P(t)$ for π^+p and π^-p elastic scattering at 100 GeV/c. The last column shows the sum of the polarization parameters for the two reactions as a test of mirror symmetry. Only statistical errors are shown.

$-t$ (GeV ²)	P_{π^+p}	P_{π^-p}	$P_{\pi^+p} + P_{\pi^-p}$
0.19±0.01	0.037±0.007	-0.023±0.008	0.014±0.012
0.25±0.05	0.025±0.004	-0.028±0.004	-0.003±0.008
0.35±0.05	0.009±0.005	-0.024±0.006	-0.015±0.010
0.45±0.05	0.003±0.007	-0.001±0.008	0.002±0.012
0.55±0.05	-0.009±0.010	-0.014±0.011	-0.023±0.016
0.65±0.05	0.005±0.014	-0.029±0.016	-0.024±0.022
0.75±0.05	-0.001±0.020	-0.018±0.023	-0.019±0.031
0.85±0.05	-0.004±0.027	0.001±0.032	-0.003±0.042
0.95±0.05	-0.016±0.036	-0.008±0.043	-0.024±0.056
1.05±0.05	-0.035±0.050	-0.025±0.061	-0.060±0.079
1.15±0.05	-0.077±0.070	0.018±0.084	-0.059±0.110
1.25±0.05	-0.097±0.085	-0.082±0.111	-0.179±0.140
1.35±0.05	0.012±0.112	-0.007±0.129	0.005±0.170

tons in the target material.

The lack of t -dependent bias was checked by fitting the t distribution of the resulting elastic events, summed over PPT enhancement, to the form $\exp(bt)$; the values obtained for b are consistent with published results.² The t distributions for the π^+p and π^-p events in the range $0.25 \leq -t \leq 0.70$ GeV² differ from published differential cross sections only by a common normalization factor.

A detailed examination of the performance of the various monitors throughout the run showed that $MT \cdot \bar{H}$ and PT were equivalent monitors of

the number of beam particles incident on the PPT. Normalization with either of them resulted in asymmetries of events in the background region which were zero within statistical errors. As an additional check, runs of the same target enhancement were used to calculate asymmetries by pretending that half of them had been taken with the opposite target enhancement; the results were again consistent with zero. The results presented here were normalized by a weighted average of $MT \cdot \bar{H}$ and PT which reduced small systematic errors associated with either monitor.

Our results for the polarization parameters in π^+p and π^-p scattering are listed in Table I and shown in Fig. 2. A t -independent systematic error of 0.005 should be added to the statistical uncertainties shown to account for monitor fluctuations.

At small $|t|$ the measured polarizations are small but nonzero, consistent with an $s^{-1/2}$ dependence. This is illustrated by the dashed curves in Fig. 2 which represent the π^+p and π^-p results of Borghini *et al.*,⁶ scaled from 10 to 100 GeV/c by s^x . Our results indicate that P_{π^+p} and P_{π^-p} are more closely mirror symmetric at 100 GeV/c than they were at 45 GeV/c.⁷ A zero occurs near $t = -0.6$ GeV², as expected. At larger $|t|$ both the π^+p and the π^-p polarizations remain small, in agreement with Regge-exchange absorption models.^{5,8}

We wish to thank R. Fuzesy for his invaluable contributions to the experiment. We also thank C. Brown, T. Droege, C. Kerns, and the staff of Fermilab for their continuing cooperation and help; S. Dhawan, S. Olsen, and M. Urban for substantial contributions to the PWC electronics;

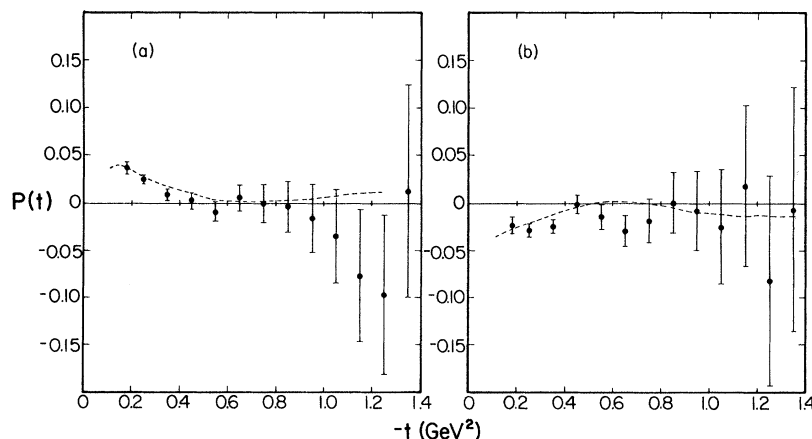


FIG. 2. Polarization parameter $P(t)$ for (a) π^+p and (b) π^-p elastic scattering. Only statistical errors are shown. The dashed curves represent the results of Ref. 6 scaled from 10 to 100 GeV/c as described in the text.

E. Sadowski for design and construction of the Cherenkov counters; and O. Fletcher for his help in maintaining the polarized target. This work was supported by the U. S. Energy Research and Development Administration,

^(a)Present address: University of Michigan, Ann Arbor, Mich. 48104.

¹C. W. Akerlof *et al.*, Phys. Rev. Lett. **35**, 1406 (1975).

²Fermilab Single Arm Spectrometer Group, Phys.

Rev. Lett. **35**, 1195 (1975).

³T. Chiu, Annu. Rev. Nucl. Sci. **22**, 255 (1972).

⁴G. F. Fox and C. Quigg, Annu. Rev. Nucl. Sci. **23**, 219 (1973).

⁵G. L. Kane and A. Seidl, Rev. Mod. Phys. **48**, 309 (1976).

⁶M. Borghini *et al.*, Phys. Lett. **36B**, 493 (1971).

⁷A. Gaidot *et al.*, Phys. Lett. **57B**, 389 (1975), and **61B**, 103 (1976).

⁸G. L. Kane, in *High Energy Physics with Polarized Beams and Targets*, AIP Conference Proceedings No. 35 (American Institute of Physics, New York, 1977), p. 43.

Non-Abelian Gauge Fields and Nonrelativistic Bound States

Frank L. Feinberg

Laboratory for Nuclear Science and Department of Physics, Massachusetts Institute of Technology, Cambridge, Massachusetts 02139

(Received 31 May 1977)

The second-quantized Coulomb-gauge Hamiltonian for any nonrelativistic system of fermions minimally coupled to non-Abelian gauge fields is derived by performing successive non-Abelian Foldy-Wouthuysen transformations. In this general formalism, a detailed analysis is made of threshold fermion-antifermion bound states in the weak-coupling limit and the form of the two-loop nonrelativistic Bethe-Salpeter kernel is determined. This kernel gives a static potential independent of the fermion mass, but only for singlet states of the gauge group.

The nonrelativistic limit of the strong interactions may be sufficiently simple to give a more tractable mathematical description than the fully relativistic theory. Furthermore, the phenomenological successes of nonrelativistic potential models¹ in describing the J/ψ family of mesons provide strong evidence that there exist physical processes dominated by the nonrelativistic strong interactions. This Letter is a first attempt to develop a consistent general formalism for systems with large quark masses, or, more generally, for any system of nonrelativistic fermions. The dynamical model is that of massless non-Abelian gauge fields minimally coupled to fermions (quantum chromodynamics). As an example of the usefulness of this formalism, fermion-antifermion bound states are discussed in perturbation theory through two loops.

The Lagrangian in first-order form is

$$L = \int d^3x \left[\frac{1}{4} F_{\mu\nu}^a F_a^{\mu\nu} - \frac{1}{2} F_{\mu\nu}^a (\partial^\mu A_a^\nu - \partial^\nu A_a^\mu + g t_{abc} A_b^\mu A_c^\nu) + \bar{\psi} (i \not{\partial} - g t^a \not{A}^a) \psi - m \bar{\psi} \psi \right]. \quad (1)$$

Fermions are in the fundamental representation of the group. The natural gauge condition for nonrelativistic systems is the radiation gauge, $\vec{\nabla} \cdot \vec{A}^a = 0$, as used by Schwinger,² who first quantized this model. Also, the first-order formalism is advantageous since it does not possess any ghosts in the radiation gauge. Imposing this gauge and transforming to the Hamiltonian gives

$$H = \int d^3x \left[\frac{1}{2} (\vec{E}^a \cdot \vec{E}^a + \vec{B}^a \cdot \vec{B}^a) + \psi^\dagger (-i \vec{\alpha} \cdot \nabla + \beta m) \psi - g \psi^\dagger \vec{\alpha} \cdot t^a \psi \cdot \vec{A}^a + \frac{1}{2} (\nabla \varphi_a) \cdot (\nabla \varphi_a) \right], \quad (2)$$

where \vec{E}^a ($\nabla \cdot \vec{E}^a = 0$) is the conjugate variable to \vec{A}^a , $B_i^a = \frac{1}{2} \epsilon_{ijk} F_{jk}^a$, and φ_a is the non-Abelian generalization of the Coulomb potential, $\varphi_a = \int d^3y D^{ab}(x, y) j_b^0(y)$. $D^{ab}(x, y)$ is an integral operator defined by

$$[\nabla^2 \delta_{ab} + g f_{abc} \vec{A}_c \cdot \vec{\nabla}] D^{bc}(x, y) = \delta^{ac} \delta^3(x - y) \quad (3)$$

and $j_a^0(x)$ is the non-Abelian charge density given by

$$j_a^0(x) = g f_{abc} \vec{E}_b \cdot \vec{A}_c + g \psi^\dagger t^a \psi; \quad (4)$$

$Q_a = \int d^3x j_a^0(x)$ are the non-Abelian charges, generators of the gauge group. To proceed to the nonrela-